INL/EXT-13-30857

KJRR-FAI Status Report of Conceptual Design Activities

N.E. Woolstenhulme
R.B. Nielson
D.B. Chapman
J.W. Nielsen
P.E. Murray
D.S. Crawford
S.D. Snow

December 2013

The INL is a U.S. Department of Energy National Laboratory
operated by Battelle Energy Alliance

INL/EXT-13-30857

KJRR-FAI Status Report of Conceptual Design Activities

N.E. Woolstenhulme
R.B. Nielson
D.B. Chapman
J.W. Nielsen
P.E. Murray
D.S. Crawford
S.D. Snow

December 2013

Idaho National Laboratory
Idaho Falls, Idaho 83415

http://www.inl.gov

Prepared for the
U.S. Department of Energy
Office of National Nuclear Security Administration
Under DOE Idaho Operations Office
Contract DE-AC07-05ID14517

KJRR-FAI Status Report of Conceptual Design Activities

INL/EXT-13-30857

N.E. Woolstenhulme
R.B. Nielson
D.B. Chapman
J.W. Nielsen
P.E. Murray
D.S. Crawford
S.D. Snow

Approved by:

N.E. Woolstenhulme — 12/20/13 — Date

R.B. Nielson — (N.E. Woolstenhulme for R.B. Nielson per email 12/20/13) — 12/20/13 — Date

M.K. Meyer — 12/20/13 — Date

CONTENTS

1. Introduction 2
   1.1 Design Inputs 3

2. Design Status 4
   2.1 Mechanical Design 4
      2.1.1 Outer Basket 4
      2.1.2 Inner Fuel Basket 6
      2.1.3 Fabrication 7
      2.1.4 Polymer Mock-up 9
      2.1.5 Material Selection 9
      2.1.6 Handling Tools 9
   2.2 Neutronics Calculations 10
      2.2.1 MCNP Model 10
      2.2.2 Calculations and Analysis 11
      2.2.3 Analytical Results 13
   2.3 Thermal Analysis 18
      2.3.1 Introduction 18
      2.3.2 Method 18
      2.3.3 Results – Safety Requirements 19
      2.3.4 Results – Test Requirements 20
   2.4 Fuel Performance Predictions 23
   2.5 Structural Analysis 25

3. Future Design Work 28

4. References 29

Abstract

The Korea Atomic Energy Research Institute has initiated the Ki-Jang Research Reactor (KJRR) project to construct a new dedicated radio-isotope production facility in the KiJang province of South Korea. The KJRR will employ a uranium-molybdenum dispersion plate-type fuel clad in aluminum. The KJRR fuel assembly design will undergo irradiation in the Advanced Test Reactor (ATR) as part of the regulatory qualification of the fuel. The Idaho National Laboratory performed a multi-disciplined conceptual design effort and found that one full-size KJRR fuel assembly can be irradiated in the ATR's north east flux trap. The analyses accomplished during the conceptual design phase are sufficient to prove viability of the overall design and irradiation campaign. Requirements for fission power can be met. The desired burnup can be achieved well within 15% depending on reactor operating availability. Mechanical design and structural analysis show that structural integrity of the irradiation test is maintained. It is recommended that future detailed design efforts be based on the concept described in this report.

Acronyms

ABAQUS	Finite Element Analysis Code
AD	Atom Densities
Al-6061	Aluminum alloy 6061
ATR	Advanced Test Reactor
ATRXS	ORIGEN2 cross section library
BOL	Beginning of Life
CRADA	Cooperative Research and Development Agreement
DNBR	Departure from Nucleate Boiling Ratio
EDM	Electrical Discharge Machine
ECAR	Engineering Calculations and Analysis Report
EFPD	Effective Full Power Days
EOL	End of Life
F&OR	Functional and Operational Requirements (INL Document Type)
FIR	Flow Instability Ratio
FORTRAN	General purpose imperative programming language
FPD	Fission Power Density
HAMP	HANARO Mini-Plate
HANARO	High-Flux Advanced Neutron Application Reactor
HFEF	Hot Fuel Examination Facility
HGR	Heat Generation Rate
HNF	Heating Normalization Factor
INL	Idaho National Laboratory
JENDL	MCNP Cross Section Library
KAERI	Korea Atomic Energy Research Institute
KJRR	Ki-Jang Research Reactor
KJRR-FAI	KJRR Fuel Assembly Irradiation
LEU	Low Enriched Uranium
MCNP	Monte Carlo N-Particle
NE	North East
NEFT	North-East Flux Trap
NFCF	Neutron Flux Conversion Factor
ORIGEN	Isotope Depletion Code
PCS	Primary Coolant System
PIE	Post Irradiation Examination
PLATE	Plate Lifetime Accurate Thermal Evaluator
PYTHON	Interactive, object-oriented, extensible programming language
SAR	Safety Analysis Report
SHF	Surface Heat Flux
U-7Mo	Binary Alloy of Uranium and 7wt% Molybdenum

KJRR-FAI Status Report of Conceptual Design Activities

1. Introduction

The Korea Atomic Energy Research Institute (KAERI) has initiated the Ki-Jang Research Reactor (KJRR) project to construct a new dedicated radio-isotope production facility in the KiJang province of South Korea. The KJRR will employ a plate-type driver fuel assembly. The fuel meat will consist of uranium 7 wt% molybdenum (U-7Mo) metallic alloy particles dispersed in a blended matrix of pure aluminum and 5 wt% silicon. The uranium enrichment will be 19.75wt% U-235 and considered Low Enriched Uranium (LEU). Aluminum alloy 6061(Al-6061) will be used as the fuel plate cladding material (see Figure 1).

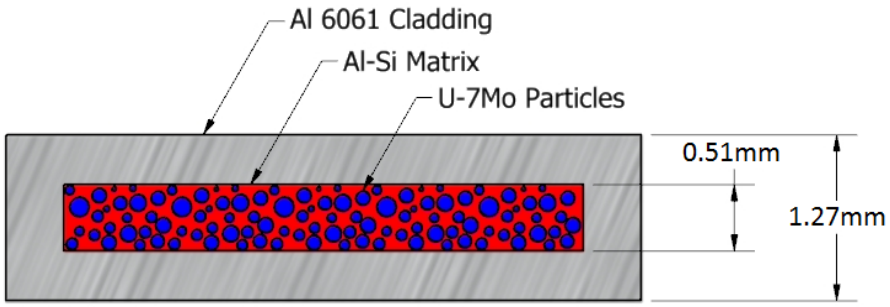

Figure 1: Fuel Plate Cross Section

Two fuel meat uranium densities of 8.0 and 6.5 g-U/cm3 will be used for the 19 interior plates and the 2 exterior plates of the KJRR fuel assembly, respectively. Fuel plate fabrication will be accomplished by hot roll bonding processes. Each of the 21 flat fuel plates will be assembled into a fuel assembly by swaging in the grooves of Al-6061 side plates giving ~620g U-235 for each KJRR fuel assembly (see Figure 2). The KJRR will receive fabricated driver fuel assemblies from a fabrication facility at the KAERI.

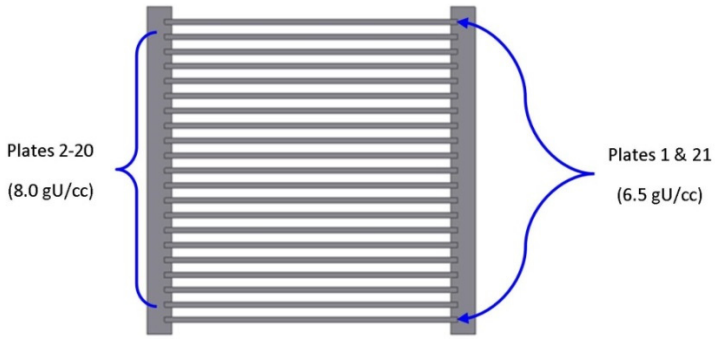

Figure 2: KJRR Fuel Assembly Top View

This fuel assembly design and fabrication technique is similar to other existing plate-type research reactor fuels, but the use of the U-7Mo dispersed in Al-Si fuel system is not. The U-7Mo dispersion fuel system has long been under development by the international community for its potential use in LEU conversion of existing research reactors[1]. While a large amount of research has taken place for this fuel system, it has not yet received generic qualification through a regulatory agency such as was accomplished for the U_3Si_2 system through the US Nuclear Regulatory Commission[2]. Hence, qualification of the KJRR fuel fabrication process and licensing the use of U-7Mo dispersion fuel in the KJRR environment will require irradiation testing of representative specimens followed by Post-Irradiation Examination (PIE).

A series of small-scale irradiation tests will be performed in the KAERI's existing HANARO research reactor in the HANARO Mini-Plate (HAMP) experiment campaigns and are discussed elsewhere[3]. The KJRR fuel qualification program will also require irradiation of a full-size driver fuel assembly. This will be performed in the North-East Flux Trap (NEFT) of the ATR with PIE in the Hot Fuel Examination Facility (HFEF); both located in the US at the Idaho National Laboratory. This campaign is termed the KJRR Fuel Assembly Irradiation (KJRR-FAI)[4].

The INL, in cooperation with the KAERI via Cooperative Research And Development Agreement (CRADA), undertook an effort in the latter half of calendar year 2013 to produce a conceptual design for the KJRR-FAI campaign. This effort demonstrated that the campaign is technically viable. This report documents the status of these conceptual design efforts while providing a framework for the future detailed design work.

1.1 Design Inputs

The KJRR-FAI concept was designed to provide data about the irradiation performance of the KJRR-fuel assembly through irradiation in the ATR, PIE in the HFEF, and as-run irradiation conditions analysis by INL personnel. The hardware was designed to provide a prototypic mechanical and thermal hydraulic configuration for one complete and unmodified KJRR fuel assembly while addressing operational and safety inputs pertaining to its use in the ATR NEFT and adjacent canal area. The fission powers and burnup distributions were designed to represent the most severe conditions of the projected KJRR design environment including a beginning of life local fission power peak corresponding to a surface heat flux at least 137 W/cm^2, and an end of life local burn-up peak of 85% ($U^{235\ Final}/U^{235\ Initial}$) depletion with respect to the initial U-235 content, both on the peak location of plate 20. The irradiation objectives, in addition to the functional, operational, and safety requirements for the campaign, were documented in a Functional and Operational Requirements (F&OR) document[5]. These requirements served as the design inputs for the KJRR-FAI conceptual design effort.

2. Design Status

2.1 Mechanical Design

The KJRR-FAI irradiation hardware is designed to adapt the KJRR fuel assembly "square" shape to fit within the cylindrical cavity of the NEFT (see Figure 3) with two assemblies referred to as the outer basket and the inner fuel basket. Two separable assemblies reduces the weight for manual handling operations in the ATR canal and vessel. Each assembly incorporates critical inputs from thermal, neutronic, and structural analysis. These features are discussed in detail in the following sections.

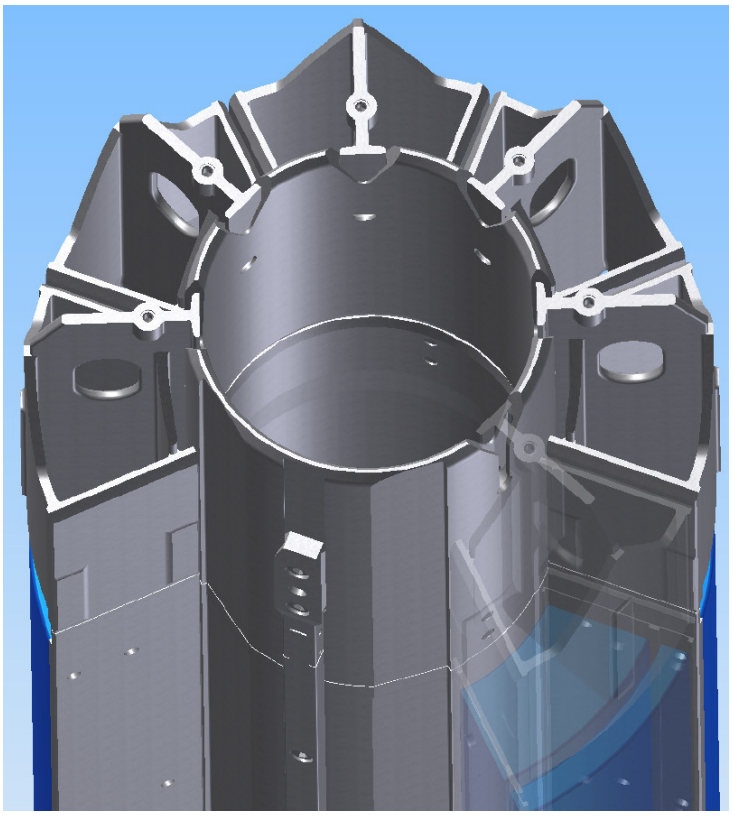

Figure 3: NEFT Baffle (empty) with ATR Driver Fuel Elements

2.1.1 Outer Basket

The outer basket is designed as an adapter from the cylindrical shape of the flux trap to the square shape of the inner fuel basket. The outer basket is designed to install into the NEFT as a simple drop-in type assembly. It is expected that the outer basket would remain in the NEFT during normal ATR outages to unnecessary minimize handling evolutions.

The outer basket is designed with locating features to ensure correct orientation of the KJRR-fuel assembly. These features engage when the outer basket is fully seated on the lower flux trap support tube assembly. The outer basket is designed with orientation notches on the top that can be visually verified from the top of the reactor.

The outer basket is designed with four flat surfaces located around the axial fueled region of the assembly. This increases the local water moderator volume in the "bypass" region between the outer basket and NEFT baffle. This serves to increase fission energy deposition in the KJRR fuel assembly; allowing fission power targets to be met with reduced North East lobe power. These features terminate prior to the upper and lower ends of the KJRR fuel meat. This suppresses the end peaks in the KJRR fuel meat in order to provide a more representative axial fission profile. See Figure 4.

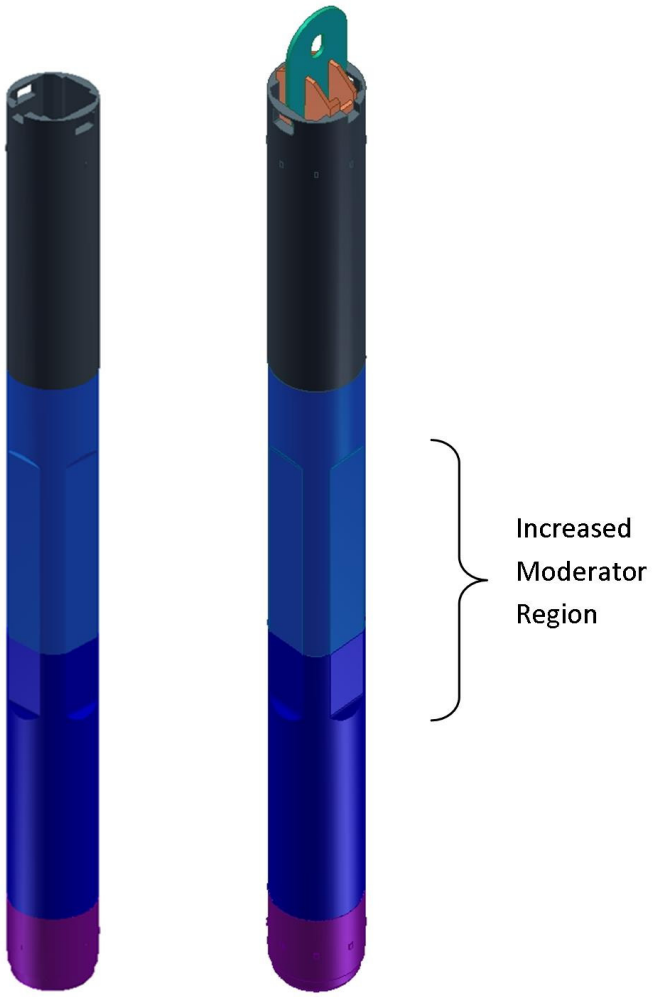

Figure 4: Outer Basket

Coolant flow is controlled by flow restrictor at the lower end of the outer basket. The design's nominal orifice diameter is based on calculated flow velocities. Flow testing will be performed by KAERI in the future to determine the orifice diameter that results in the desired flow rate of 7.2 m/s through the fuel coolant channels. See Figure 5.

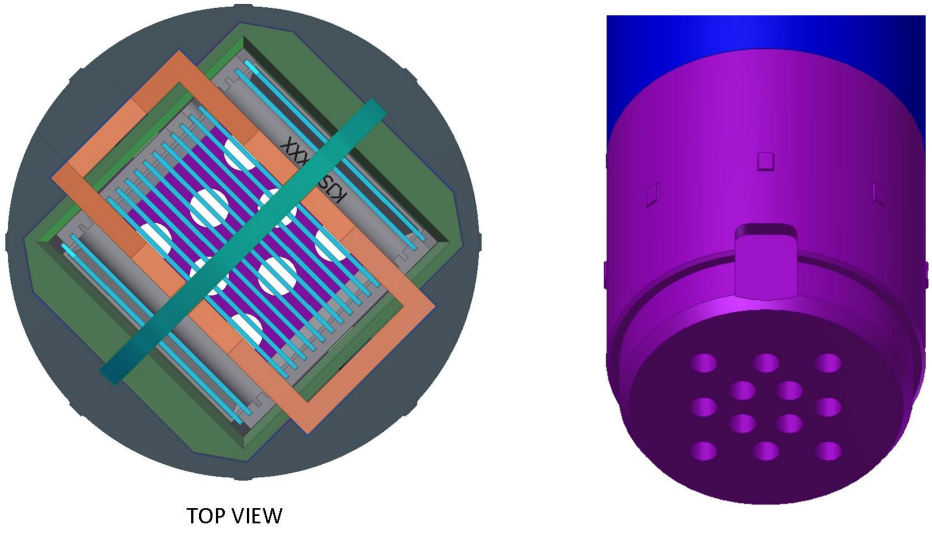

Figure 5: Outer Basket Flow Restrictor Design

2.1.2 Inner Fuel Basket

The inner fuel basket is designed to locate the KJRR fuel assembly within the outer basket. The inner fuel basket can be removed from the outer basket (with the KJRR fuel assembly inside), after each cycle for visual exams in the canal area during outages, see Figure 6. The inner fuel basket chamfered features prevent improper installation rotationally. Like the outer basket, a large notch feature enables visual verification of rotation. The inner fuel basket is designed with robust aluminum plates to protect the fuel plates from damage during handling while exposing the fuel assembly's sideplates for natural convection removal of decay heat should the assembly become oriented horizontally during handling.

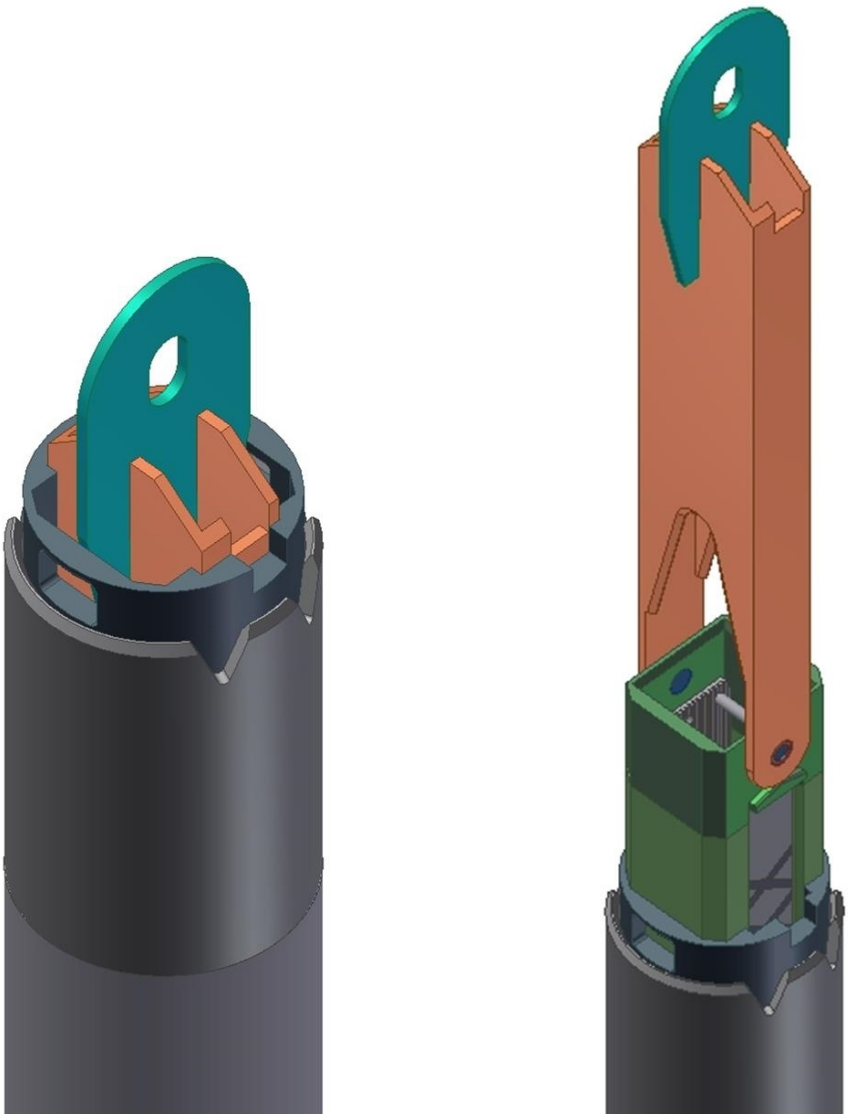

Figure 6: Inner Fuel Basket Extraction from NEFT Baffle

The inner fuel basket is designed with a handle that can be rotated out of the way to remove the KJRR-fuel assembly. The handle attaches with welded stainless steel pins so that the pin captures the handle and can rotate independent of the handle and the inner fuel basket; minimizing the risk for binding. A handle stop is included as part of the inner fuel basket. See Figure 7.

Figure 7: Inner Fuel Basket Design

2.1.3 Fabrication

Since it is infeasible to fabricate the intricate inner cavity geometry of the outer basket and inner fuel basket using a conventional lathe or mill, a wire Electric Discharge Machine (wire EDM) is the primary piece of equipment considered in the design of the outer basket. An aluminum mock-up with similar dimensions to one of the outer basket sections was fabricated by the INL machine shop using a Sodick Model AQ750LH wire EDM to verify that the basket pieces could be fabricated. The pieces for the inner fuel basket can be fabricated using a combination of conventional machining and wire EDM. See Figure 8 and Figure 9.

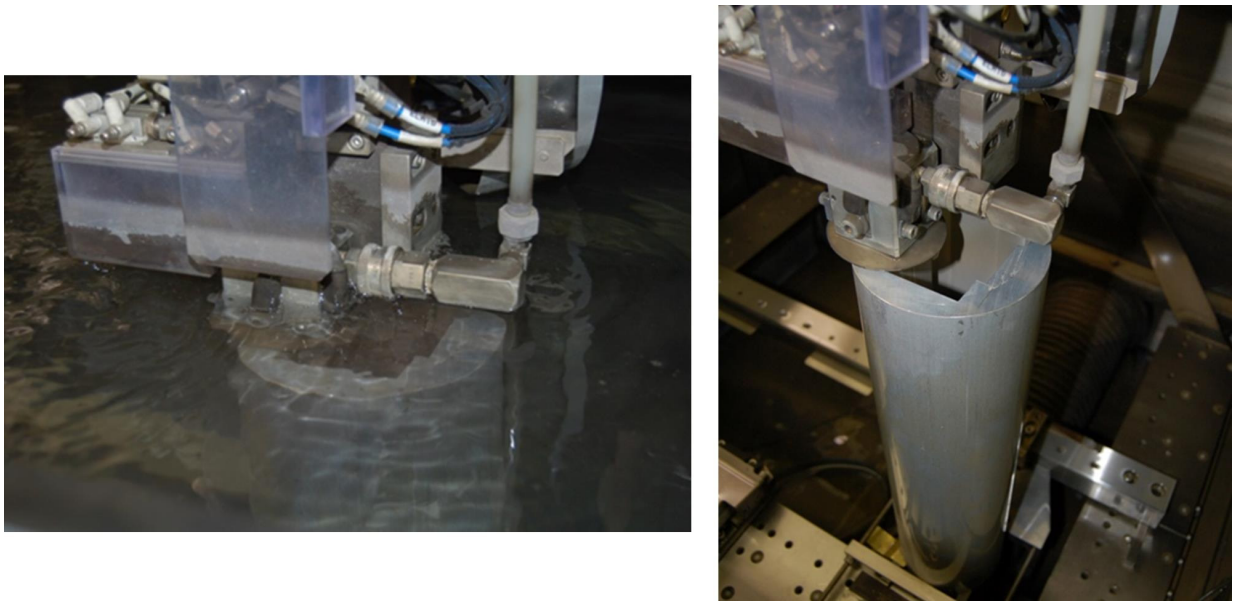

Figure 8: Wire EDM

Figure 9: Aluminum Segment Mock-Up

2.1.4 Polymer Mock-up

To better understand how these parts will be assembled, handled, and fit together, a 3D printer was used to make a mock-up assembly. These pieces were shorter in length than the final design, but were otherwise built at full-scale. As a result of this mockup, several design improvements were made including the stop for the inner fuel basket handle (discussed in Section 2.1.2), a chamfer on the bottom edge of the fuel basket to assist assembly in the reactor vessel, and inclusion of visible notch on the top of both the inner fuel basket and outer basket to correctly orient the assembly when installed. See Figure 10.

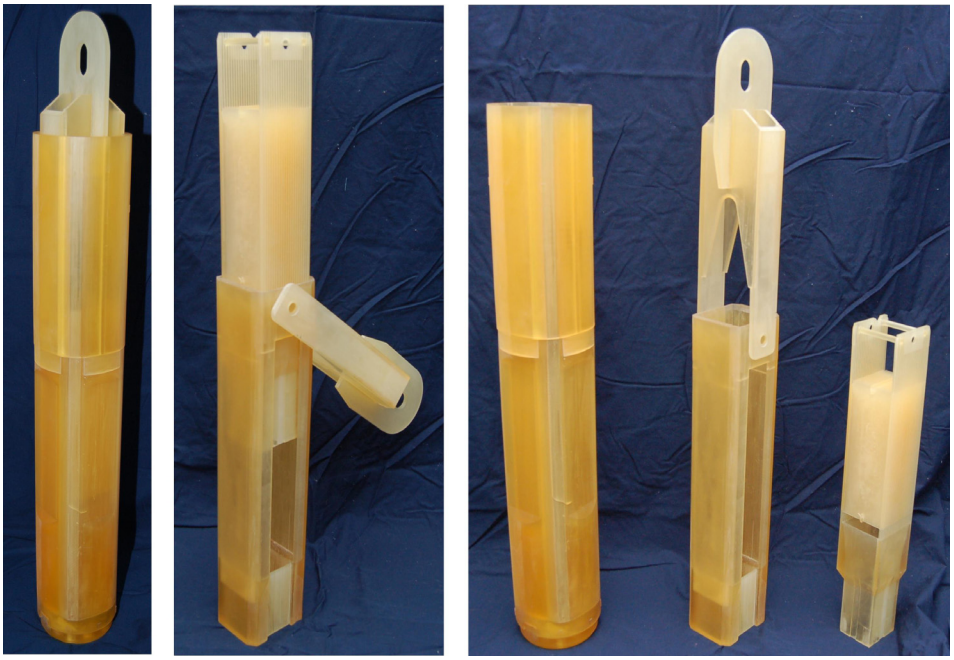

Figure 10: Pictures of Polymer Mock-Up

2.1.5 Material Selection

The inner fuel and outer baskets are designed to be fabricated primarily from 6061-T6 aluminum. Aluminum was chosen based on its low neutron absorption cross section and lighter weight (compared to stainless steel); making it easier for personnel to handle the assemblies in the ATR canal and vessel. Stainless steel is used for the pin on the inner fuel basket handle to provide a stronger attachment point and prevent galling between the pivoting handle and the pin. Stainless steel is also easier to weld and maintains a higher strength than aluminum weld joints. The stainless pin is designed to be welded to a stainless washer capturing the handle. Stainless dowel pins are used to align the four pieces of the outer basket as these can be purchased in highly accurate sizes with a tolerance of ±0.005mm.

2.1.6 Handling Tools

The inner fuel and outer baskets are designed to be handled using ATR standard positive latching hook tools Figure 11. These tools use a simple hook design with a locking pin to prevent any accidental separation of the hook from the assembly being moved. Since the KJRR fuel assembly itself must be handled by the two holes on the sideplates, a special handling tool must be used. KAERI will deliver a KJRR fuel assembly handling tool to the INL, along with dummy fuel assemblies, for handling rehearsals during future design phases. The INL will either use the KAERI tool as-is, or perform design modifications to adapt it for use in the ATR facility, based on the outcomes of these handling rehearsals.

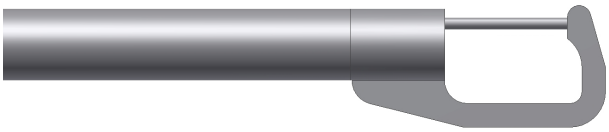

Figure 11: ATR Positive Latching Hook Tool

2.2 Neutronics Calculations

The KJRR-FAI was modeled in an ATR full core MCNP model. The MCNP model was used to determine heat rates in the fuel plates, calculate 1-group cross-sections, and determine the neutron flux in the design. The MCNP model was coupled with ORIGEN2 Version 2.2 using a PYTHON script to determine burn-up using MCNP updated cross-sections and calculated MCNP flux where compositions are then transferred back into the MCNP model to determine heat rates at each burn-up time step.

2.2.1 MCNP Model

The KJRR-FAI was modeled using the hardware design described in Section 2.1. An MCNP diagram of the model is shown in Figure 12 and Figure 13. Each of the fuel plates were modeled using nominal dimensions and material compositions. The outer holder assembly is a cylindrical component with a square cavity. The cylinder reduces down to an outer square configuration to increase water +/- 25 cm from core center leaving approximately 5 cm of active fuel meat on the ends in the cylindrical portion of the holder. Figure 13 displays the additional water volume due to the outer square profile. This design feature reduces water moderator on the ends and reduces axial end peaking in the KJRR fuel assembly. Fuel compositions and atom densities used in the MCNP model are summarized in Table 1 and Table 2.

The standard MCNP cross-section data libraries[6][7] and the JENDL-3.2 cross-section libraries[8] were used to perform all MCNP evaluations for the KJRR-FAI. The ORIGEN2 library ATRXS[9] and the design-specific MCNP-generated cross-sections were used to calculate the depletion of the KJRR fuel plates.

Table 1: Material compositions for KJRR fuel meat

	Fuel Meat							
Plates	Width (mm)	Length (mm)	Thickness (mm)	Volume (cc)	U Mass (g)	U-235 Mass (g)	Mo Mass (g)	Al Mass (g)
1&21	62	600	0.51	18.972	123.3	24.4	9.3	30.4
2-20	62	600	0.51	18.972	151.8	30.0	11.4	25.6

Table 2: KJRR atom densities (atoms/b-cm)

Plates	U-235	U-238	Mo	Al	Total
1&21	3.2891E-03	1.3196E-02	3.1701E-03	3.5816E-02	5.5471E-02
2-20	4.0481E-03	1.6241E-02	3.9017E-03	3.0174E-02	5.4365E-02

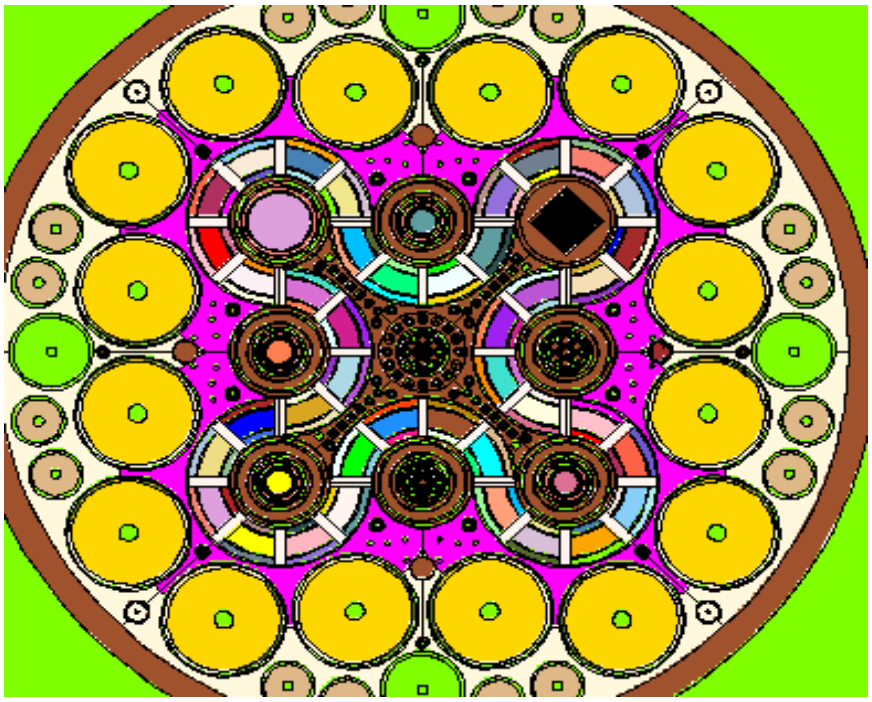

Figure 12: ATR MCNP Full-Core Physics Model

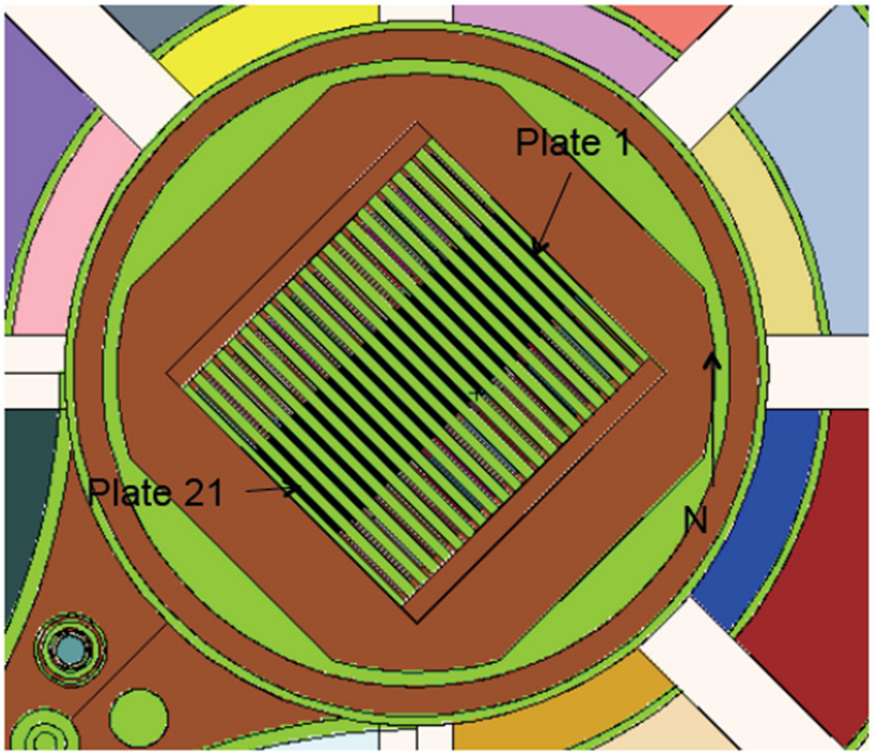

Figure 13: KJRR-FAI in the ATR MCNP Model (NEFT)

2.2.2 Calculations and Analysis

The MCNP-calculated Heat Generation Rate (HGR) profiles were evaluated using the results from an ATR three-region detailed MCNP full core physics model. The ORIGEN2-calculated U-235 depletions were evaluated using the results from ATR three-region detailed MCNP full core physics model evaluations and associated ORIGEN2 runs. The calculated fission densities were also evaluated using the

results from ATR three-region detailed MCNP full core physics model evaluations and associated ORIGEN2 runs.

2.2.2.1 MCNP Heat Generation Rate Calculations

The MCNP type 7 fission energy deposition tally has units of MeV/g per source neutron. The f7:n tally tallies all fission energy generated in the fissile material. The f7 tally results are used to calculate fission HGR values for material compositions. MCNP reports tally results normalized per source particle. The Heating Normalization Factor (HNF) used to calculate either fission heating or neutron/prompt photon heating due to fission neutrons is given by equation (1).

$$HNF = \left(\frac{2.43\ fission\ neutrons}{fission}\right)\left(\frac{fission}{200\ MeV}\right)\left(\frac{1 \times 10^6 W}{MW}\right)$$

$$HNF = 1.215 \times 10^4 \frac{fission\ neutrons - W}{MeV - MW} \quad (1)$$

The fission and neutron/prompt photon HGR values are calculated using the MCNP type 6 or 7 tally results, the HNF, and the ATR core power. The fission heating rate (FHR) is calculated using equation (2).

$$FHR = \left(type\ 7\ neutron\ tally\ \frac{MeV}{g - fission\ neutron}\right)\left(1.215 \times 10^4 \frac{fission\ neutrons - W}{MeV - MW}\right)(Core\ Power\ MW)$$

$$FHR = (f7)(HNF)(Core\ Power) = \frac{W}{g} \quad (2)$$

$$NPPHR = \left(type\ 6\ photon\ tally \frac{MeV}{g - fission\ neutron}\right)\left(1.215 \times 10^4 \frac{fission\ neutrons - W}{MeV - MW}\right)(Core\ Power\ MW)$$

For fueled compositions, the Fission Power Density (FPD) and the Surface Heat Flux (SHF) are calculated using the FHR values, the fuel density, and the fuel thickness. FPD is calculated using equation (3) and SHF is calculated using equation (4).

$$FPD = \left(FHR\ \frac{W}{g}\right)\left(\rho \frac{g}{cc}\right) = \frac{W}{cc} \quad (3)$$

$$SHF = \left(FPD \frac{W}{cc}\right)\left(\frac{fuel\ thickness\ cm}{2\ sides\ per\ plate}\right) = \frac{W}{cm^2} \quad (4)$$

2.2.2.2 MCNP Neutron Flux Calculations

MCNP reports tally results normalized per source particle. The MCNP type 4 flux tallies for neutrons have units of neutrons/cm^2 per fission neutron. The f4:n flux tally results are used to generate neutron flux values which are used with ORIGEN2 for depletion calculations. The Neutron Flux Conversion Factor (NFCF) is defined by equation (5).

$$NFCF = \left(\frac{2.43\ fission\ neutrons}{fission}\right)\left(\frac{fission}{200\ MeV}\right)\left(\frac{MeV}{1.60219 \times 10^{-13} J}\right)\left(\frac{J}{W - sec}\right)\left(\frac{1 \times 10^6 W}{MW}\right)$$

$$NFCF = 7.583 \times 10^{16} \frac{fission\ neutrons}{MW - sec} \quad (5)$$

The neutron flux values are calculated using the MCNP tally type 4 results, the NFCF, and the ATR core power. The neutron flux is calculated using equation (6).

$$\Phi_{neutron} = \left(type\ 4\ neutron\ tally \frac{neutrons}{cm^2 - fission\ neutron}\right)\left(7.583 \times 10^{16} \frac{fission\ neutrons}{MW - sec}\right)(Core\ Power\ MW)$$

$$\Phi_{neutron} = (f4)(NFCF)(Core\ Power) = \frac{neutrons}{cm^2 - sec} \quad (6)$$

2.2.2.3 ORIGEN2 Depletion Calculations

The depletion of U-235 is calculated using initial U-235 Atom Densities (AD) for the fuel compositions as well as results of the ORIGEN2 burnup evaluations for the fuel compositions. ORIGEN2 depletes the fuel compositions as a function of irradiation time. The % depletion of U-235 at the end of irradiation is calculated using equation (7).

$$\%\ Depletion\ U235 = \frac{AD\ U235_{initial} - AD\ U235_{final}}{AD\ U235_{initial}} \times 100 \quad (7)$$

The fission density is calculated by determining the difference in actinide atom densities at each time step. The fission density is therefore determined by the following equation:

$$Fission\ Density = AD\ Actinides_{Initial} - AD\ Actinides_{final} \quad (8)$$

2.2.3 Analytical Results

The MCNP coupled with ORIGEN methodology was used to determine Beginning of Life (BOL) heat rates and determine the amount of time required to reach a burn-up of 85% in Plate 20. Each plate was divided into 10 axial and 4 transverse nodes of equal volume. The plates were irradiated in the model with a North East (NE) Lobe Power of 21 MW for 100 days followed by an additional 150 days for 23 MW. Table 3 provides a summary of the BOL heat rates on Plate 20. The U-235 depletion on Plate 20 is presented in Table 4 and Table 5 for 200 and 250 Effective Full Power Days (EFPD), respectively. The 200 and 250 EFPD calculations predict a peak U235 burnup of 78.84% and 87.42%, respectively; falling within -8% and +3% of the target burnup of 85%. A summary of the heat rates and burn-up rates on all plates is shown in Figure 14 through Figure 17.

Table 3: BOL heat flux for Plate 20

Horizontal/Vertical (cm from edge)	Plate 20 Heat Flux (W/cm^2)			
	0.78	2.33	3.55	5.43
3	150.02	141.78	143.04	152.14
9	158.46	147.05	148.19	158.76
15	168.60	158.36	158.29	170.74
21	174.45	163.81	164.21	177.50
27	179.63	167.53	166.19	182.67
33	180.52	168.03	165.88	180.94
39	176.91	165.25	167.32	180.29
45	174.54	160.34	162.41	174.08
51	163.14	153.26	152.58	165.28
57	158.94	151.00	151.46	161.29

Table 4: Plate 20 U-235 burn-up at 200 days of irradiation

Horizontal/Vertical (cm from edge)	Plate 20 U-235 Burn-up 200 EFPD			
	0.78	2.33	3.55	5.43
3	71.28%	69.88%	70.20%	71.93%
9	73.46%	71.25%	71.68%	73.58%
15	75.97%	74.20%	74.12%	76.32%
21	77.20%	75.70%	75.67%	77.95%
27	78.13%	76.35%	76.05%	78.84%
33	78.50%	76.69%	76.12%	78.59%
39	77.76%	76.03%	76.34%	78.46%
45	77.22%	74.80%	75.15%	77.31%
51	74.85%	72.88%	72.80%	75.18%
57	73.76%	72.42%	72.68%	74.28%

Table 5: Plate 20 U-235 burn-up at 250 days of irradiation

Horizontal/Vertical (cm from edge)	Plate 20 U-235 Burn-up 250 EFPD			
	0.78	2.33	3.55	5.43
3	80.89%	79.92%	80.17%	81.50%
9	82.90%	81.17%	81.60%	82.99%
15	85.04%	83.82%	83.73%	85.36%
21	86.09%	85.15%	85.07%	86.71%
27	86.89%	85.65%	85.42%	87.42%
33	87.20%	85.93%	85.50%	87.25%
39	86.58%	85.42%	85.63%	87.12%
45	86.11%	84.36%	84.66%	86.20%
51	84.08%	82.61%	82.59%	84.38%
57	83.15%	82.22%	82.44%	83.56%

The currently planned schedule window for the KJRR-FAI includes five normal ATR cycles 158B through 162B. These cycles are planned for EFPD irradiation times as shown in Table 6. The ATR has historically operated at 75%-85% of the planned EFPD due to unforeseen equipment failures and other complications. Table 6 displays cumulative EFPD at 75% and 85% of planned operation corresponding to 206 EFPD and 233 EFPD with 79% and 84% U-235 peak burn-up, interpolated from the peak results in Table 4 and Table 5, respectively. These projections indicate that KJRR-FAI conceptual design is well poised to achieve its End of Life (EOL) burnup target of 85% when irradiation for five cycles; especially when considering that these projections were performed using a large node size (60mm X 6.2mm) where peaking within the node will be greater. The primary concern for KJRR reaching its burnup target would occur if it were irradiated for fewer than five normal ATR cycles. Four cycles of irradiation, for example would result in 70% to 75% peak burnup.

Table 6: Plate 20 Peak Burnup per Cycle EFPD

NE Lobe Power	**21MW**	**21MW**	**23MW**	**23MW**	**23MW**		
Cycle	**158B***	**160A**	**160B***	**162A**	**162B***		U-235 burn-up
planned EFPD each	57	46	57	57	57		
planned EFPD total	57	103	160	217	274		
85% of planned, EFPD total	48	88	136	184	233	→	84%
75% of planned, EFPD total	43	77	120	163	206	→	79%

*Cycles currently planned at 60 EFPD, but emergent considerations make 57 EFPD a better estimate

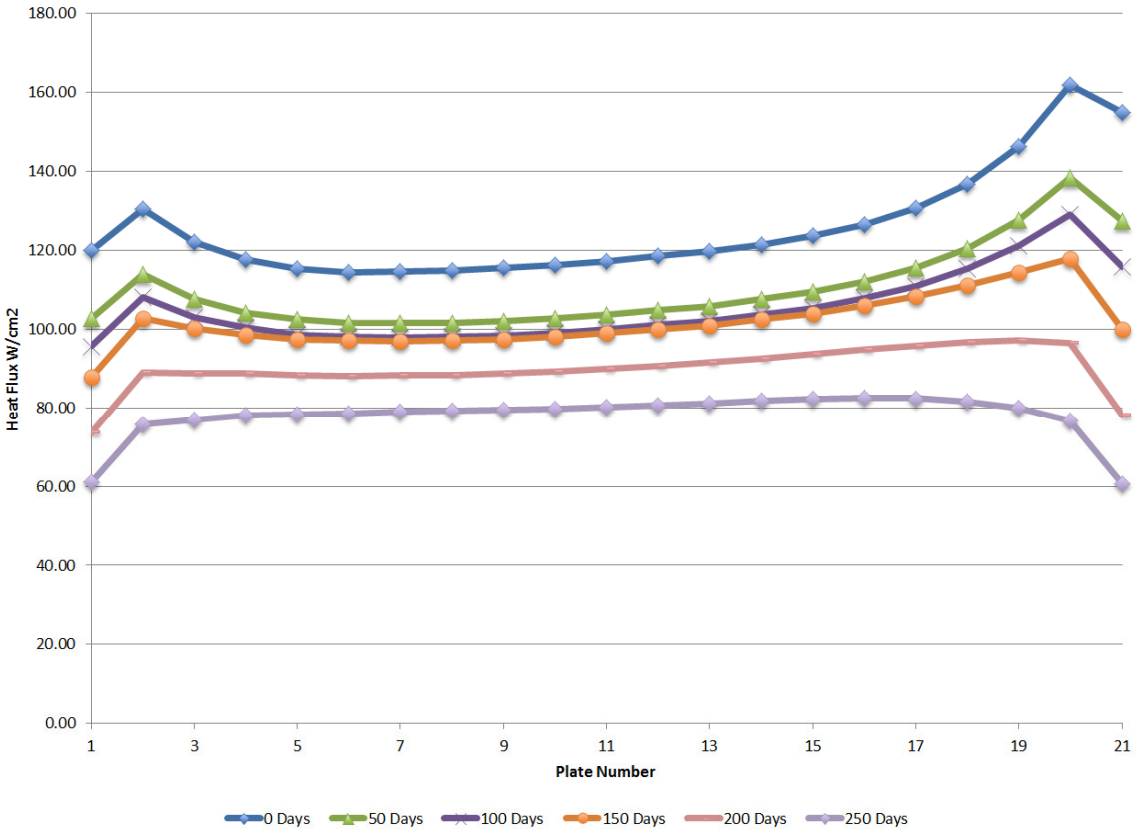

Figure 14: Average plate heat flux during irradiation

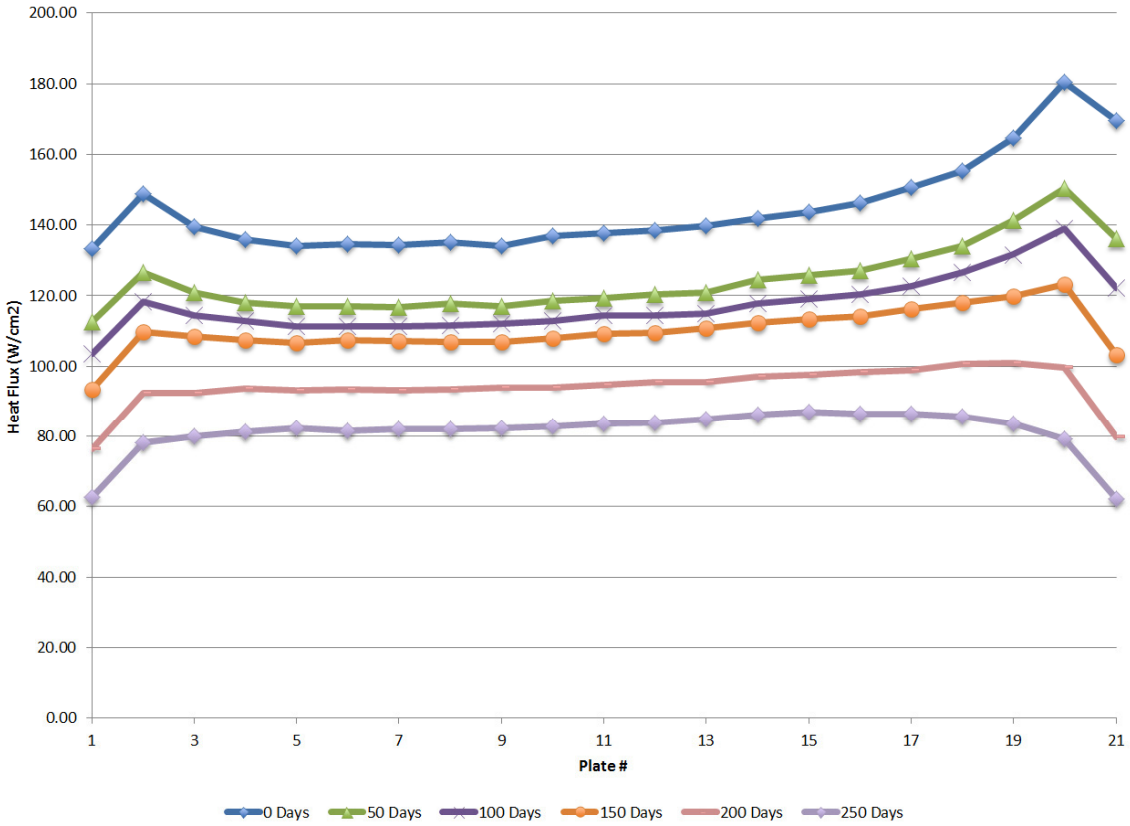

Figure 15: Peak node on plate heat flux during irradiation

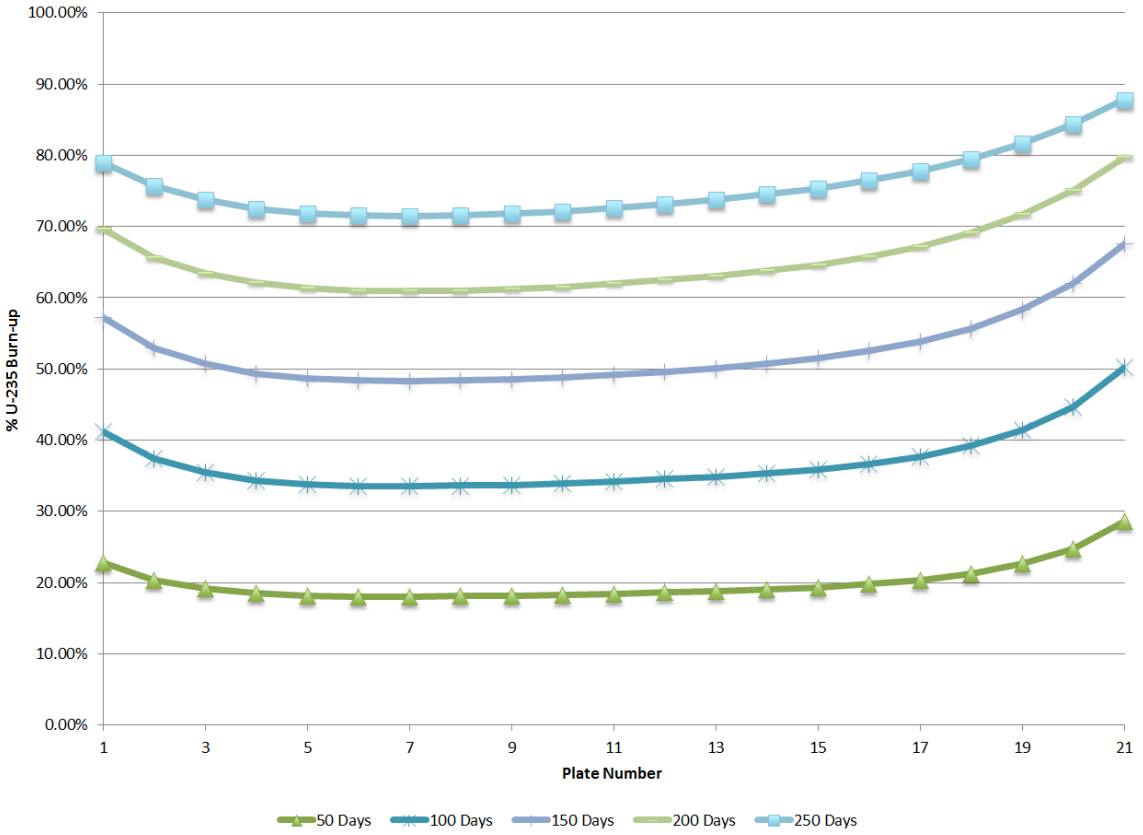

Figure 16: Average plate burn-up as a function of irradiation time

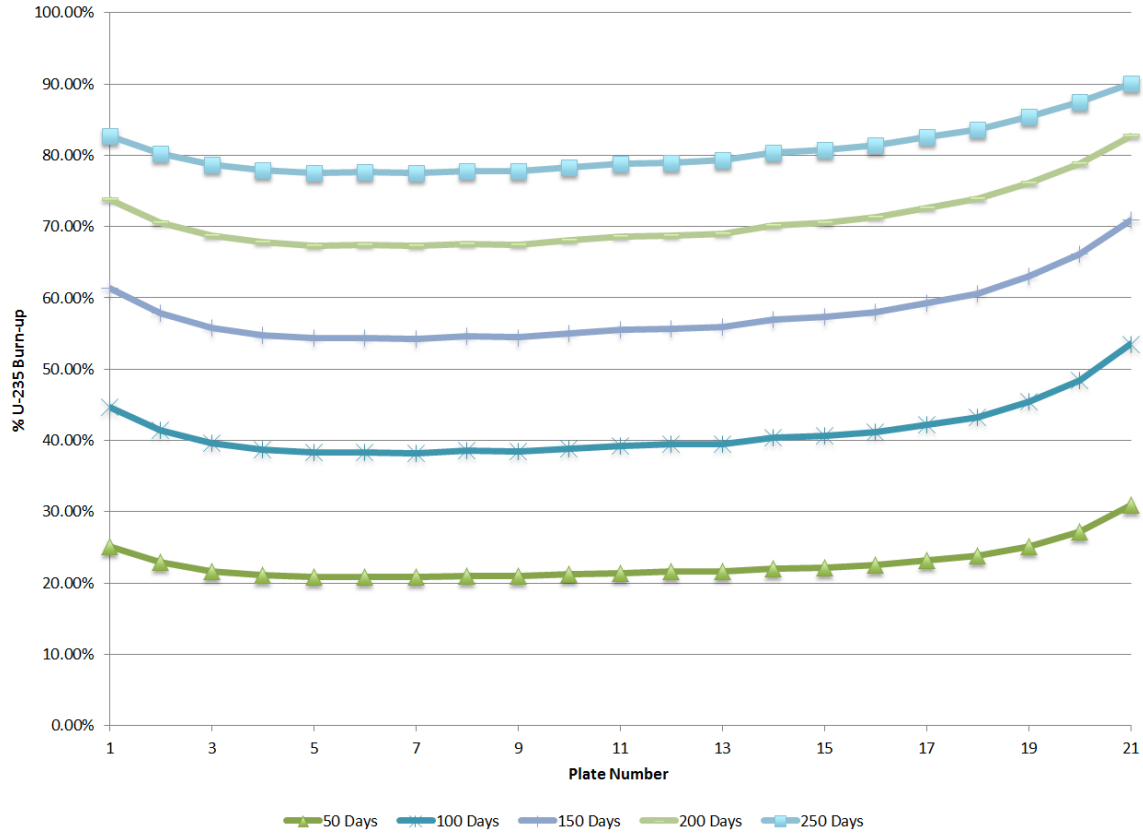

Figure 17: Peak node on plate burn-up as a function of irradiation time

2.2.3.1 ATR Lobe Power

The KJRR fuel assembly will add a significant amount of power to the ATR reactor. The MCNP models were used to determine the fraction of heat produced in the KJRR fuel assembly relative to the ATR NE Lobe power. A summary of the KJRR total heat rate with ATR NE Lobe Power heat rates are reported in Table 7.

Table 7: KJRR contribution to the NE Lobe Power

Days	KJRR Source Power (MW)	% of Lobe Power
0	1.59	7.58%
25	1.60	7.64%
50	1.46	6.96%
75	1.40	6.66%
100	1.34	6.36%
125	1.39	6.06%
150	1.32	5.72%
175	1.24	5.39%
200	1.16	5.06%
225	1.09	4.72%
250	1.01	4.38%

2.3 Thermal Analysis

2.3.1 Introduction

A thermal evaluation was performed to demonstrate that the KJRR-FAI design in the NEFT will comply with the thermal-hydraulic safety requirements of the ATR Safety Analysis Report (SAR). The SAR requires that the safety requirements be met in the case of a loss of commercial power accident with primary coolant pump coast-down to emergency flow. The thermal safety evaluation was performed at 31 MW NE lobe power to encompass the expected range of operating power during a standard cycle. A second evaluation was performed at 21 MW NE lobe power to provide best-estimate beginning-of-irradiation test conditions. These results show that the required limits on maximum temperature and heat flux will be met.

2.3.2 Method

The ABAQUS[10] model included all 21 fuel plates, 2 side plates, baskets, and coolant channels. The coolant inlet temperature and pressure was modelled at 52°C and 2.48 MPa with a core pressure drop of 0.53 MPa. A flow restriction plate containing 12 orifice holes (each ~11.5 mm in diameter) was modelled below the end fitting to obtain a desired coolant velocity in the fuel plate coolant channels equal to 7.2 m/s. Coolant flow was calculated to be 1416 liters/min through the test assembly, 15 liters/min in the bypass channels between inner and outer baskets, and 288 liters/min between the outer basket and flux trap baffle. This gave a total coolant flow through the NEFT of 1719 liters/min. The MICE experiment was previously irradiated in the NEFT with coolant flows from 1616 to 1828 liters/min[11]. This provides confidence that the ATR Primary Coolant System (PCS) can support the flow rates needed for the KJRR-FAI.

The KJRR fuel plate materials were modeled with a U-7Mo alloy dispersed in Al-5Si, 6061 aluminum cladding, and an oxide film produced by corrosion of aluminum in water. The uranium loading density was modelled with 8.0 g/cc in the 19 interior plates and 6.5 g/cc in the 2 exterior plates. Thermo-physical properties of U-Mo/Al dispersion fuel were obtained from Table 7, Table 11, and Figure 9 in International Journal of Thermophysics 28(5), 2007[12]. Properties of 6061 aluminum and its in-reactor corrosion layer were obtained from INL report PG-T-91-031[13]. Properties of compressed water were obtained from Perry's Chemical Engineers' Handbook[14].

The important phenomena affecting fuel plate thermal conditions were fission power, fission density, coolant hydrodynamics, fuel plate thermal properties, oxide growth at the cladding surface, and growth of the interaction layer between fuel particles and aluminum matrix. Although the low thermal conductivity of aluminum oxide layers and the U-7Mo-Al interaction layers lead to a decrease in the effective thermal conductivity of irradiated fuel plates, supporting calculations discussed in Section 2.4 indicated that the maximum fuel temperature will occur at the beginning of irradiation because the decrease in fission power more than compensates for the decrease in fuel thermal conductivity. Therefore, the following calculations assumed BOL conditions to be the most limiting. The plates were modelled with 5 micron surface oxide layers to represent prefilmed boehmite layers.

The heating rates obtained from the neutronic analysis discussed in section 2.2 were input to the ABAQUS analysis using a FORTRAN subroutine. The coordinates of the MCNP grid cells were used in the ABAQUS subroutine to identify the grid cell in which a particular finite element is located, and the heating rate in the element was set to the fission power in the corresponding MCNP grid cell.

The thermal load case evaluated in this report included steady-state operation at 31 MW, with an 8.5% increase in power to account for lobe power uncertainty, a 2.5% increase in fission power due to the fuel loading limit, and a localized increase in fission power due to fuel homogeneity limits (16% or 27% depending on location in the fuel plate). The fuel loading limit and fuel homogeneity limits were obtained from Section 3.1.2 in the test requirements report KJ-374-KN-442-010[15]. Safety factors on coolant flow included a 25% reduction that bounds the pump coast-down transient. An additional thermal load case evaluated steady-state operation at 21 MW without any safety factors. In both cases, nominal fuel zone dimensions were assumed.

A finite element, steady-state heat transfer analysis of the test assembly and primary coolant channels were performed using ABAQUS. The 8-node linear brick element was used to model the solid components. The 8-node forced convection brick element was used to model the primary coolant with a prescribed mass flow rate. The model geometry of the test assembly is shown in Figure 18. The parts are color coded: fuel plates are red, side plates are orange, end fitting is gold, inner basket is green, and outer basket is cyan.

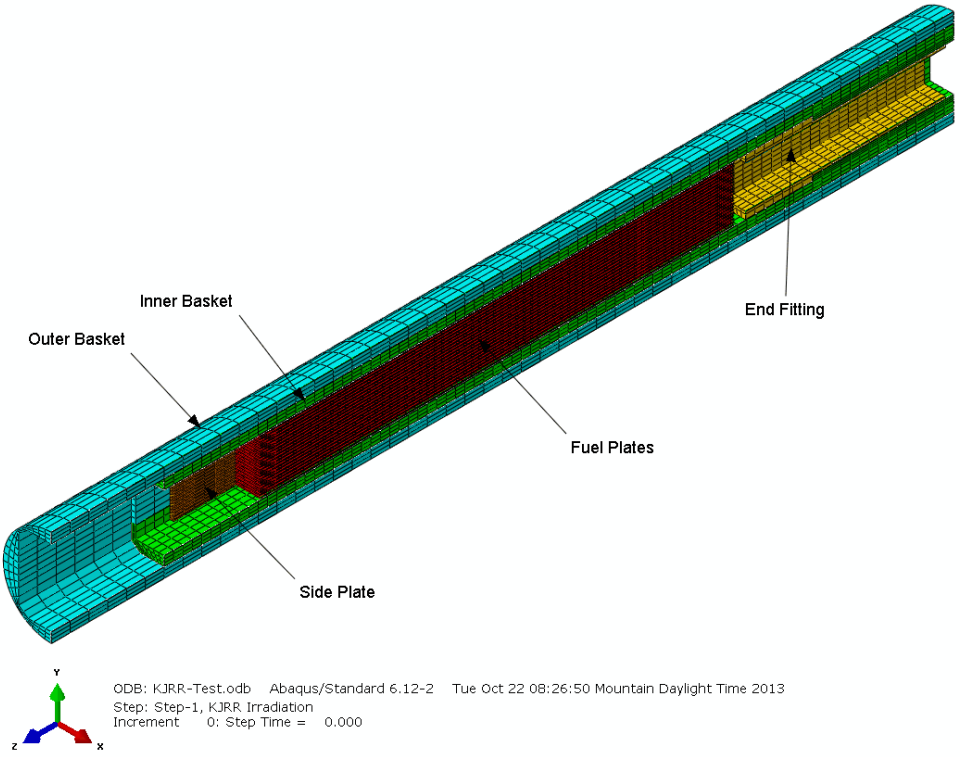

Figure 18: Model geometry of the test assembly

2.3.3 Results – Safety Requirements

An evaluation was performed for a loss of commercial power accident with primary coolant pump coast-down to emergency flow; assuming the reactor is initially operating at 31 MW lobe power and the PCS is initially operating with 2-pumps. The flow and power transients resulting from a reactor trip at low vessel inlet pressure were obtained from INL report EDF-4953[16]. A steady-state analysis at 31 MW power with an 8.5% power measurement uncertainty bounded the expected range of operating power, and a 25% reduction in primary coolant flow bounded the pump coast-down transient.

A contour plot of the temperature of the cooling channels at pump coast-down conditions is shown in Figure 19. In this figure, the model is oriented with the reactor coolant flowing from left to right. The maximum temperature of the primary coolant is 120°C.

A contour plot of the heat flux at the fuel plate surfaces at pump coast-down conditions is shown in Figure 20. The maximum heat flux at the outer surface was calculated at 348 W/cm^2. The Critical Heat Flux (CHF) for forced convection was obtained from the Savannah River Laboratory data (DP-1306)[17] as 1585 W/cm^2. The ratio of critical heat flux to maximum heat flux, Departure from Nucleate Boiling Ratio (DNBR), is 4.5. The Savannah River Laboratory CHF correlation was obtained from data on aluminum heaters cooled by a water annulus with coolant velocities from 4.5 m/s to 18 m/s, and is applicable to subcooling greater than 25°C.

The core outlet pressure at pump coast-down conditions was modelled as 1.79 MPa. The coolant saturation temperature at this pressure is 209°C. Since the coolant inlet temperature is 52°C, the

temperature rise to saturation is 157°C. The actual maximum temperature rise of the primary coolant is 68°C. The ratio of the maximum allowable temperature rise to the actual temperature rise, Flow Instability Ratio (FIR), is 2.3.

2.3.4 Results – Test Requirements

ABAQUS simulations of plate temperature and heat flux at the beginning of irradiation at 21 MW NE lobe power are shown in Figure 21 and Figure 22. Plate 20 has the highest fission power, and the maximum fission power occurs at the edges of the plate. The maximum value of heat flux occurs at the side edge of plate 20 (the second plate closest to core center) where the fission power is greatest. The maximum value of fuel temperature occurs at the bottom edge of plate 20 where the coolant temperature is greatest. The maximum values of temperature and heat flux are 134°C and 185 W/cm^2, respectively. The limits on maximum temperature and maximum heat flux are 200°C and 200 W/cm^2 (Sections 3.2.1 and 3.2.2 in KJ-374-KN-442-010[15]). These results show that the required limits on maximum temperature and maximum heat flux are met.

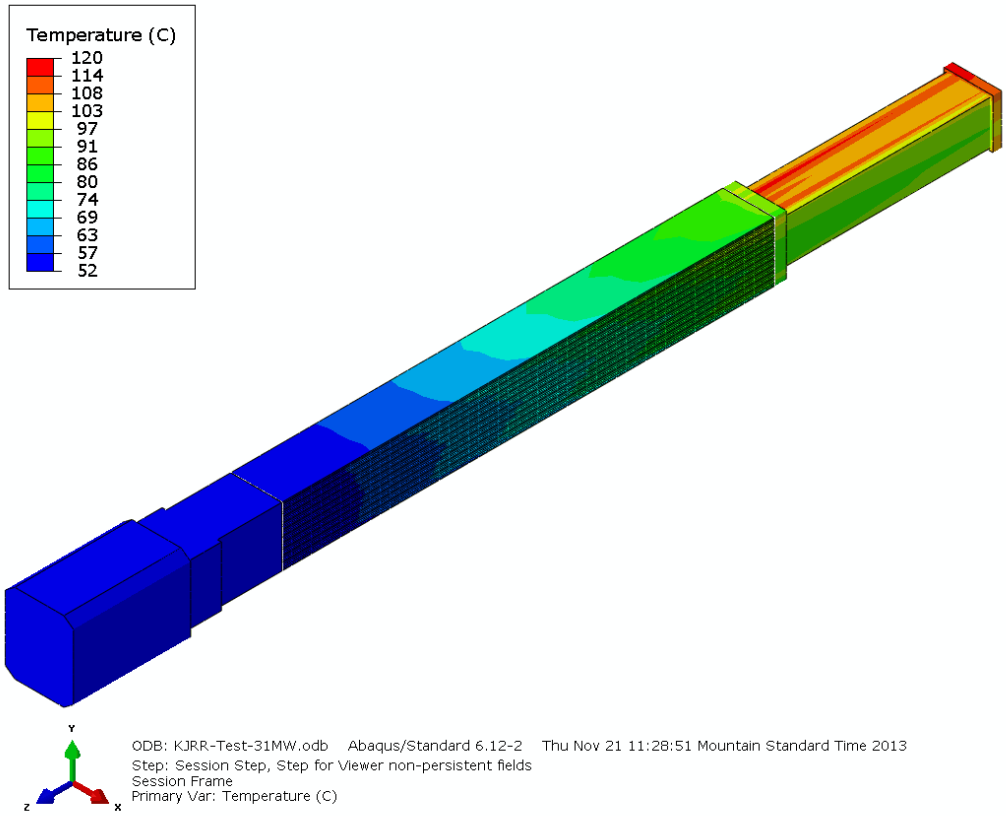

Figure 19: Coolant temperature at 31 MW

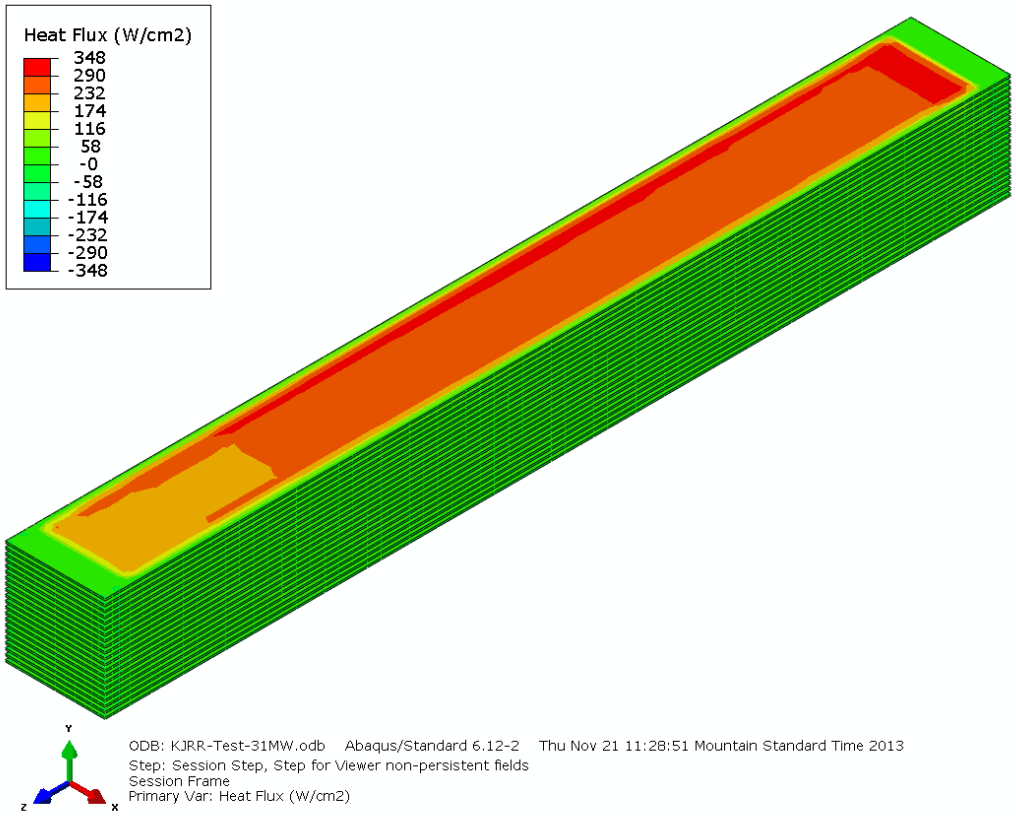

Figure 20: Plate surface heat flux at 31 MW

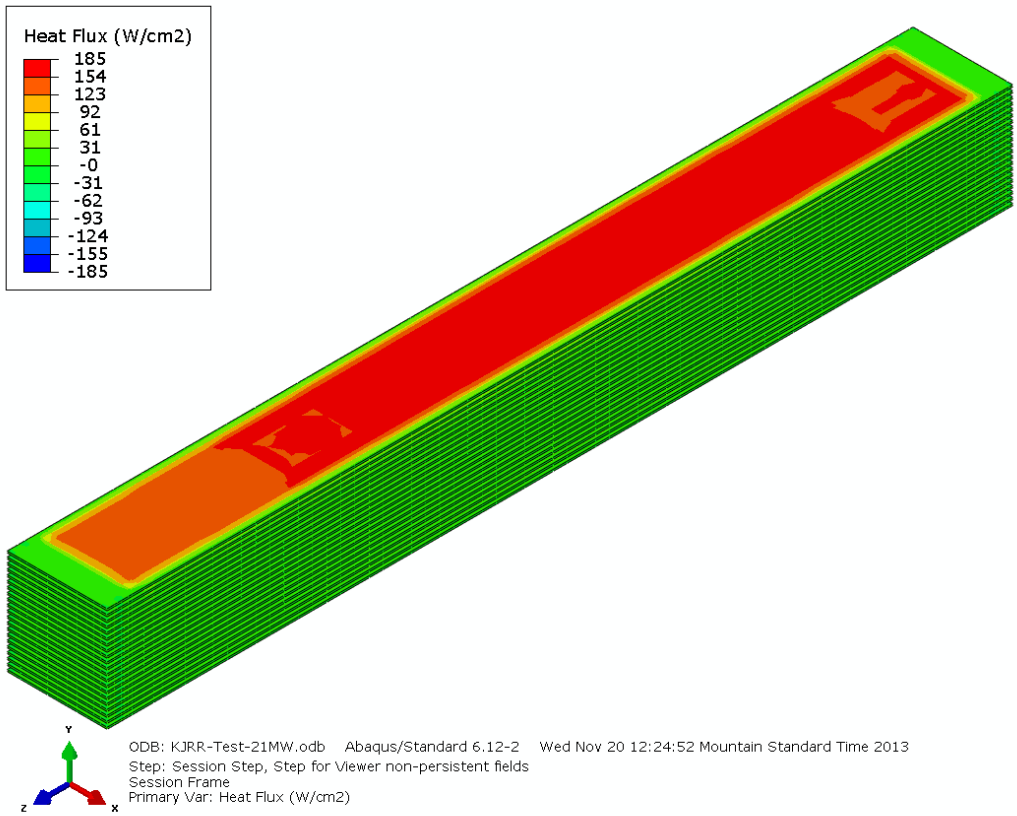

Figure 21: Plate surface heat flux at 21 MW

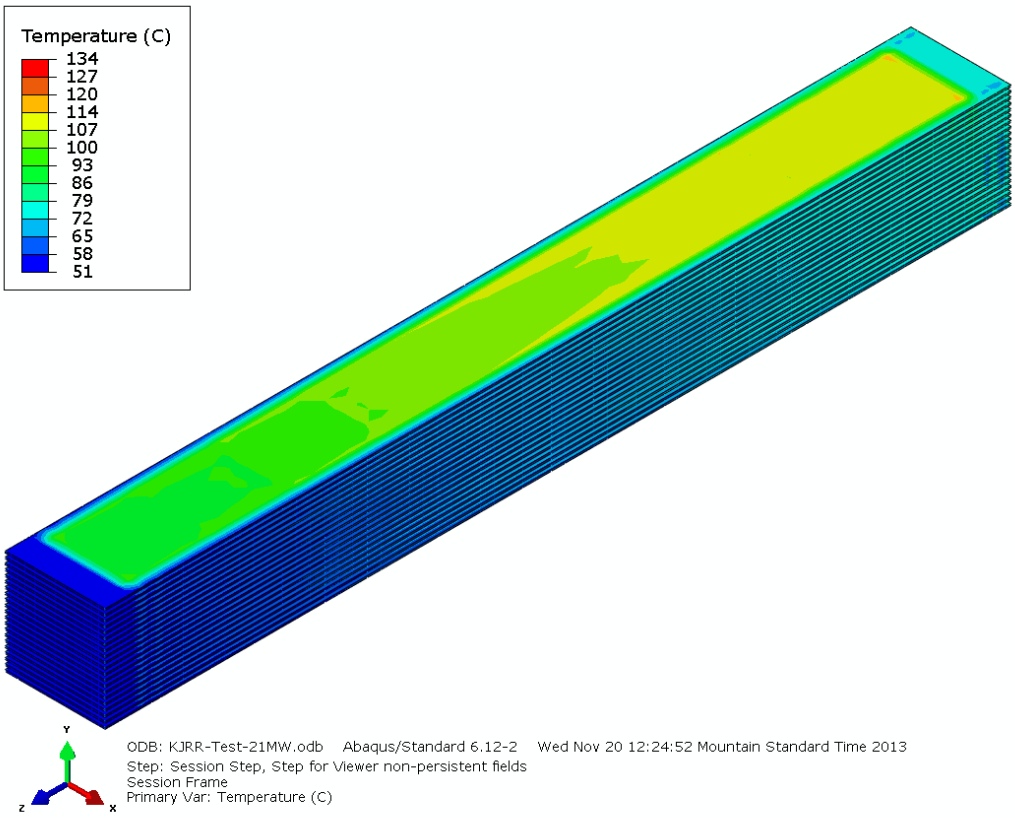

Figure 22: Plate temperature at 21 MW

2.4 Fuel Performance Predictions

A preliminary analysis of the KJRR-FAI was performed in the PLATE-2.0 code. Conditions corresponding to plate #20 were analyzed. The input conditions for the KJRR preliminary PLATE calculations are as follows:

- 250 EFPD
- Interpolated the MCNP power source terms onto the PLATE mesh of 15 nodes in the x-direction (thickness), 8 nodes in the y-direction (width) and 32 nodes in the z-direction (length)
- Fuel type is U-7Mo
- Dittus-Boelter convection coefficient
- Coolant flow rate 7.2m/s
- 2-phase thermal conductivity model
- Linear boehmite layer growth model up to 10µm
- U-7Mo-Al fuel matrix chemical reaction layer model, stoichiometry of 7 Al to 1 U atom
- Assumed dispersed fuel particle size distribution to be 72.7% with a diameter 190µm, 27% with a diameter of 125µm and the balance 20 µm in diameter.

The PLATE mesh allowed for only Al cladding to be contained into the outer control volumes, this closely matched the physical dimensions of the KJRR fuel assembly. Like ATR driver fuel assemblies, the KJRR fuel assembly will receive boehmite prefilming for irradiation in the ATR PCS. Accordingly, the ATR modified Griess oxide growth model was used for this analysis. The Dittus-Boelter convection correlation for turbulent flow was used to calculate the convection heat transfer coefficient (h). This correlation provides a preliminary h value to get a reasonable idea of the temperatures of the KJRR plate. Figure 23, Figure 24, and Figure 25 show selected output from the PLATE analysis. These results are preliminary and should be considered an estimate only of the fuel behavior trends that the KJRR-FAI might follow in the ATR.

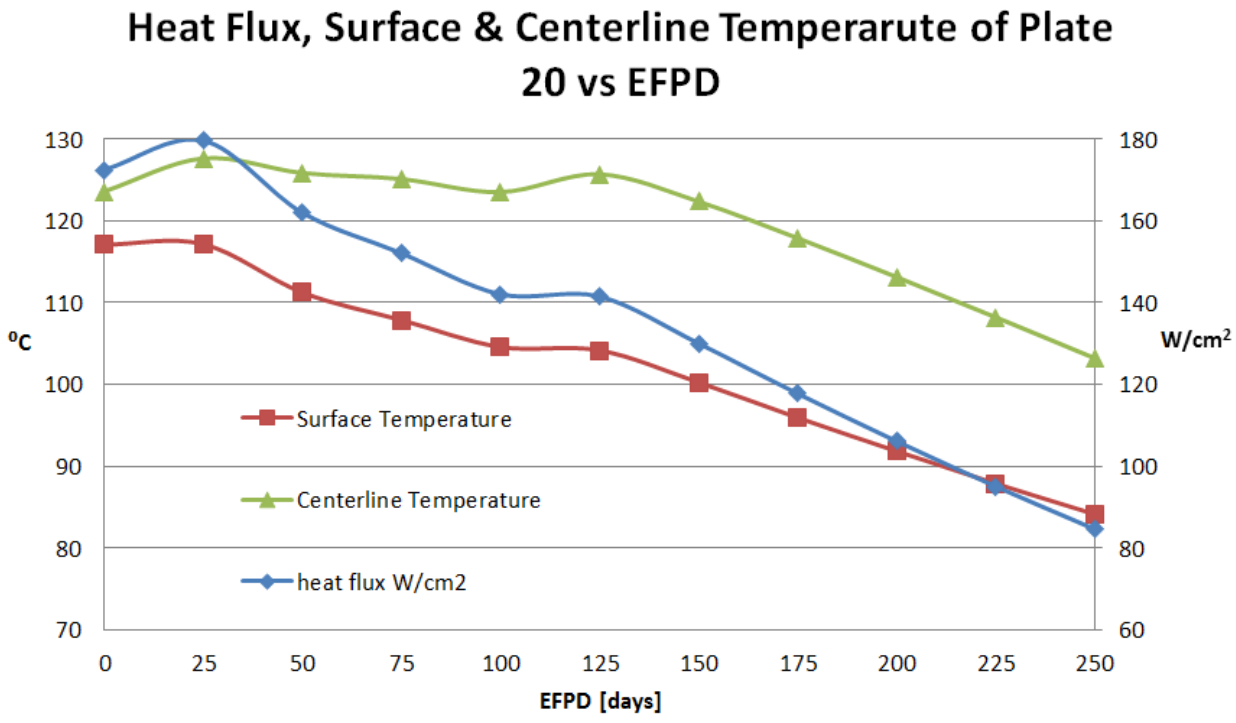

Figure 23: Average heat flux and temperature* along the centerline and surface of plate 20

*Due to the PLATE model's use of a conservative convective heat transfer correlation and lack of 3-dimensional heat conduction through the cladding, the trends shown likely overestimate the heat flux and temperatures.

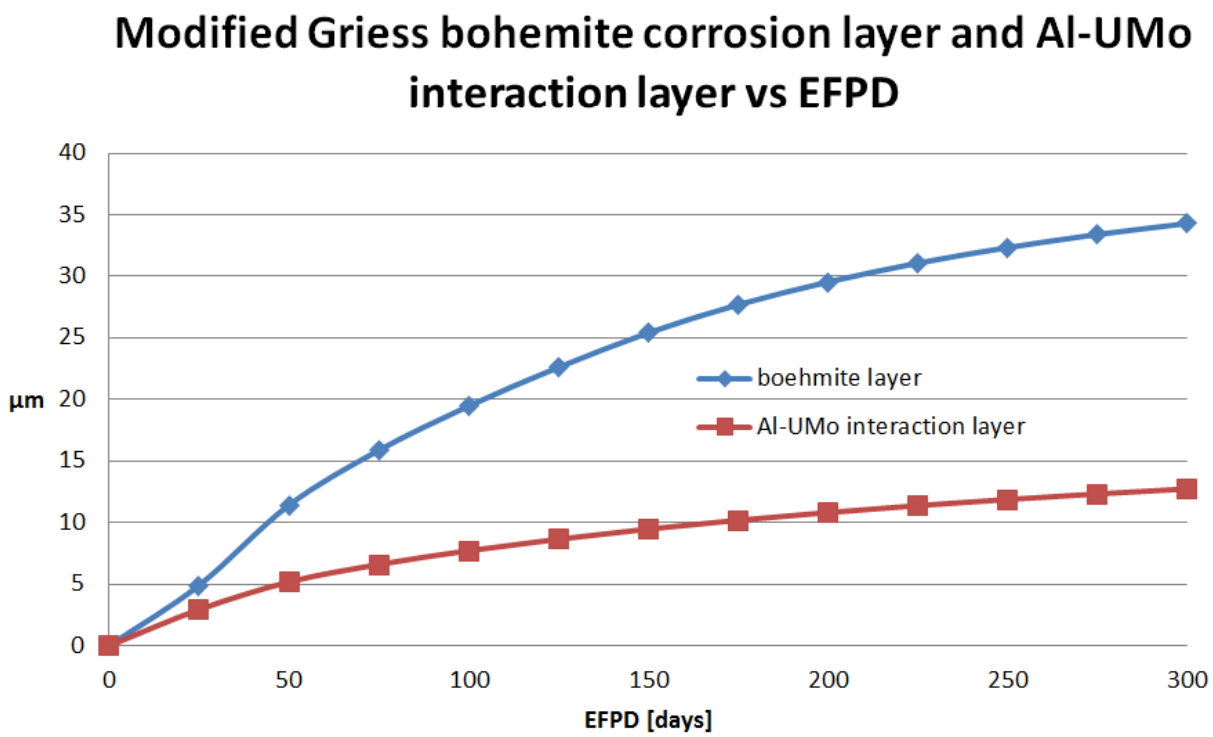

Figure 24: Plot of the average growth of the U-7Mo-Al reaction layer

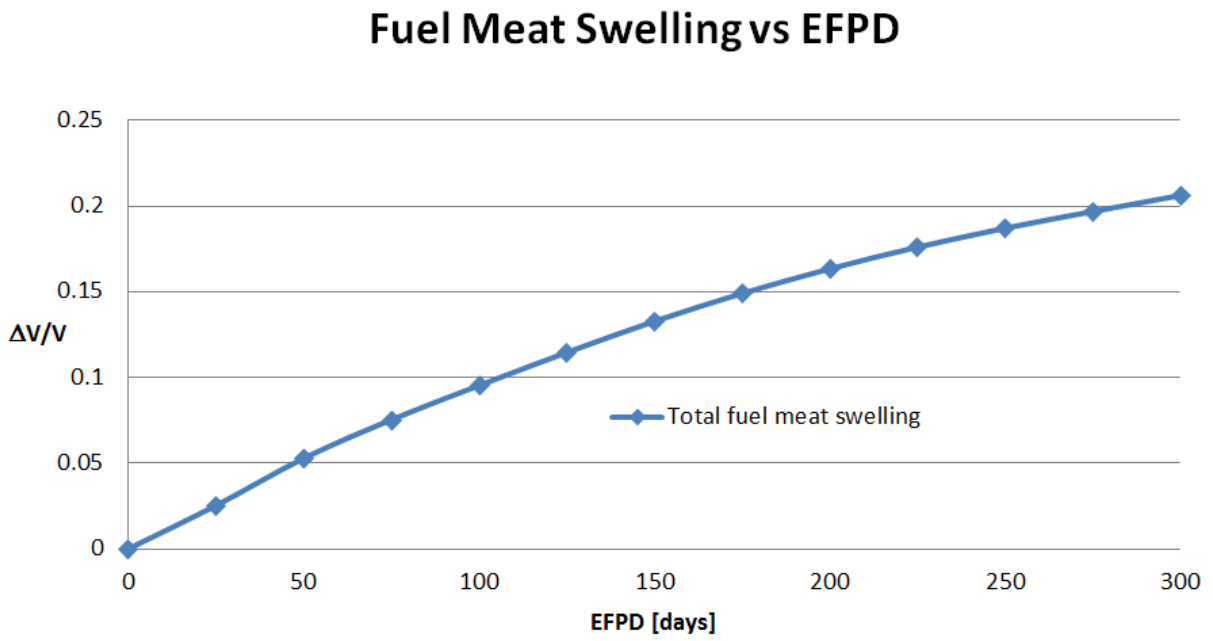

Figure 25: Plot of the fuel meat swelling versus the irradiation time in days

2.5 Structural Analysis

A structural evaluation model of the standard fuel assembly was generated using the ABAQUS software. This model used continuum elements to represent the side plates, fuel plates, fixing bars, end fixture, combs, and pins. Figure 26 shows the structural finite element model of the fuel assembly. The purpose of the structural evaluations was to show that the standard fuel assembly, inner fuel basket, and outer basket would remain structurally sound during irradiation within the ATR vessel and while handled before and after irradiation.

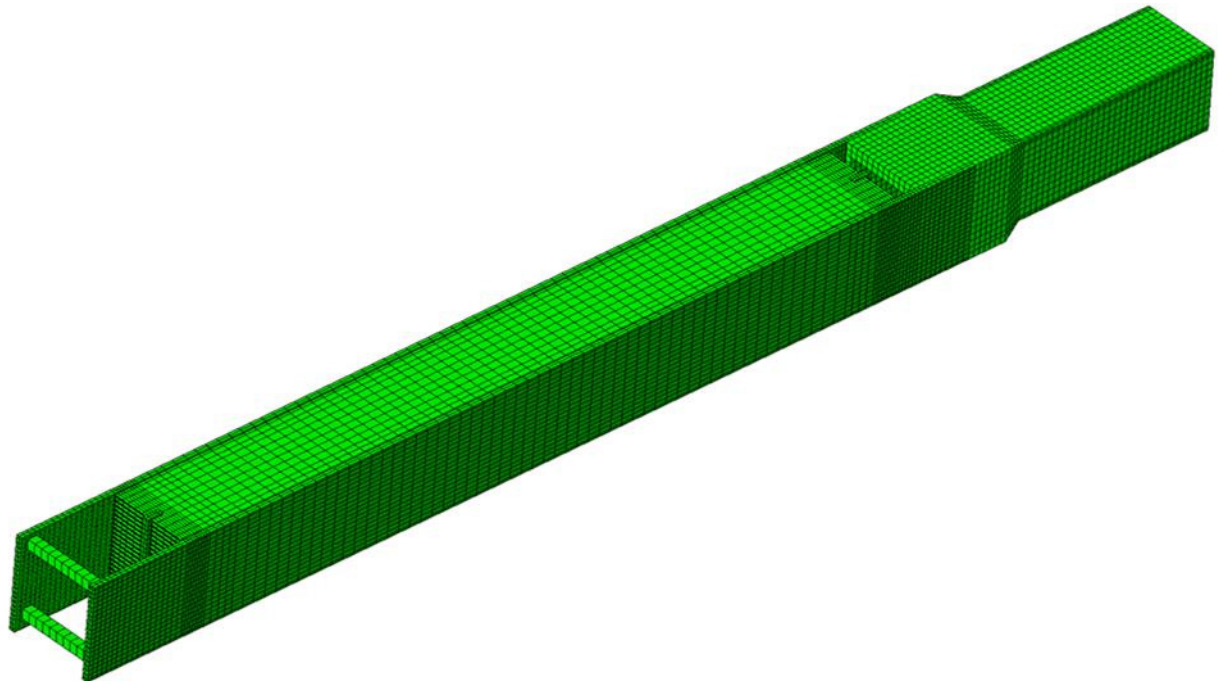

Figure 26: Structural model of the standard fuel assembly

The response of the fuel assembly to reactor operating conditions is due to temperatures (mapped from the thermal ABAQUS model), reactor vessel pressure, pressure drop across the reactor core, flow drag forces, and flow-induced vibrations.

The thermal evaluation considered two loadings; a 21MW thermal case to represent the normal operating environment in the ATR, and a 31MW thermal case that takes into account uncertainties in fuel loading, safety factors, etc., and was considered an enveloping case. The structural model was evaluated for the 21MW thermal case only, and the stress results are shown in Figure 27. The majority of the fuel plates experienced stresses well below the material yield strength, while a localized area (at a swage joint) sees stresses at the yield strength. Side plates, fixing bar, and end fitting stresses are all well below the material yield strength. Stresses due to the reactor pressure and flow drag loadings are small. This preliminary evaluation of the fuel assembly indicates that structural stability will be maintained.

Flow-induced vibration potential was also evaluated. First, coolant flow parallel to the fuel plates was evaluated. The maximum amplitudes of vibration were calculated, using the Burgreen method, at 0.043mm and 0.053mm, for the 21MW and 31MW thermal cases respectively, subjected to the 7.2 m/s normal operating coolant flow velocity. These maximum amplitudes of vibration are not insignificant - but are small, and are not expected to be a concern because the associated stresses are low.

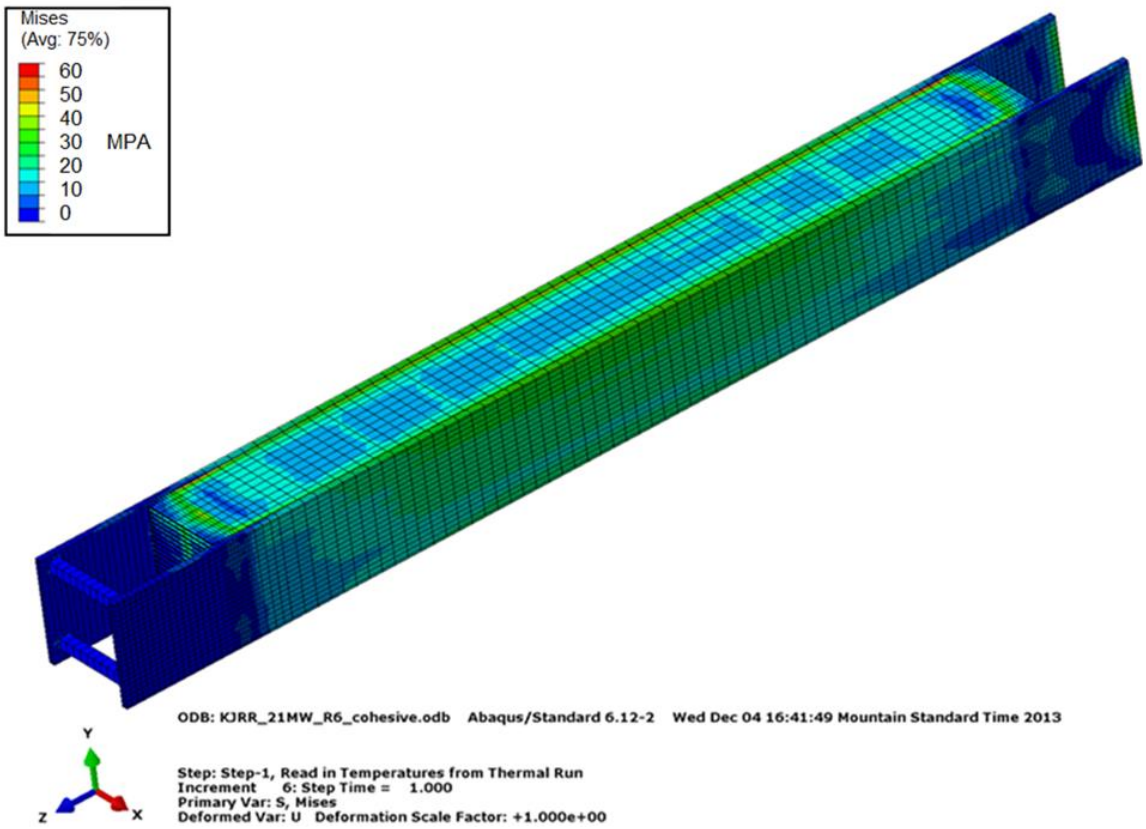

Figure 27: Structural model stress results (combs and end fitting not shown)

Second, the coolant flow off the trailing edge of the fuel plates was evaluated since it has significant clear volume available for the forming of flow vortices that could load the plates. However, the vortices that could potentially develop off of the twenty-one fuel plate trailing edges are likely to interfere with each other and not result in coherent, cyclical loadings of a significant magnitude. Regardless, assuming that coherent vortices could form, the frequency of vortex shedding from the 7.2 m/s normal operating flow velocity was calculated at greater than 1100 Hz using the Blevins method. The fundamental frequency of the fuel plates in coolant was calculated at just over 200 Hz. (Note that the sixth vibrational mode of a fuel plate was calculated at about 500 Hz.) Therefore, the vortex shedding frequency is well away from lower vibrational modes. Should synchronization with much higher vibrational modes of the fuel plates occur, it is expected to result in small vibrational displacements. Vibrations due to vortex shedding are therefore a negligible concern for this fuel assembly.

Third, the Miller critical coolant parallel flow velocity, below which value a fuel plate should not collapse, was also calculated. The results indicated a critical flow velocity of 16.6 m/sec. for the 21MW thermal load case, and 15.8 m/sec. for the 31MW thermal load case. These critical flow velocities exceed the normal operating flow (7.2 m/s) significantly, and collapse of the fuel plates is not expected to occur.

In summary, the above calculations showed that vibrations of the fuel plates within the assembly should not be significant under the 7.2 m/sec. normal flow velocity, for the 21MW and 31MW thermal load cases. However, these calculations were based on empirical equations developed for specific geometries that were not the same as in this fuel assembly. Since these fuel plates are thin and flat, and the normal coolant velocity is significant, the plan to perform hydraulic flow testing of the KJRR-FAI assembly is warranted.

Limited preliminary hand calculations of the inner fuel basket and the outer basket were also performed and have shown that the designs are expected to be adequate for handling purposes and under the normal operating loadings in the ATR vessel. Analytical models of these baskets (see Figure 28) have been generated.

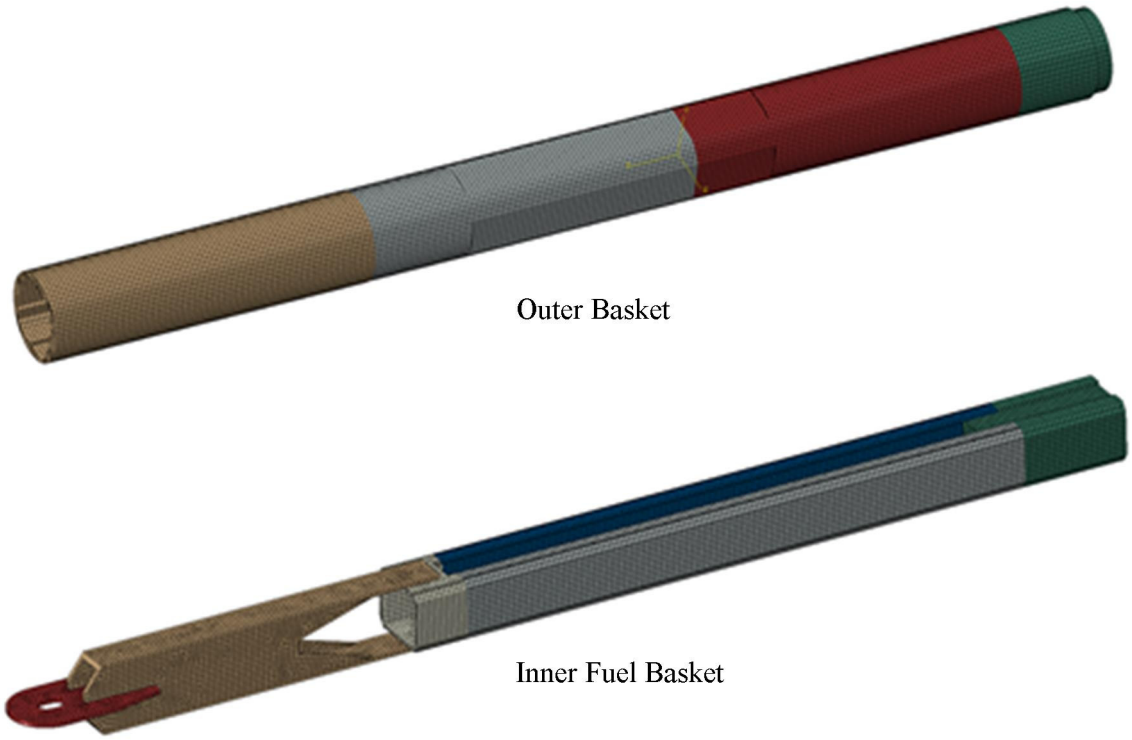

Figure 28: Structural models of outer basket and inner fuel basket

3. Future Design Work

The irradiation assembly described in section 2.1 was technically drafted into engineering drawings with modification to use a bolt-on orifice plate for fabrication and use in hydraulic flow testing performed by KAERI. These drawings and technical inputs to the flow testing effort are described elsewhere[18]. Hydraulic flow testing efforts should be accomplished as soon as possible in case design changes are required to address results from the flow test. Once flow testing is completed, the flow testing hardware should be shipped to the INL along with dummy KJRR fuel assemblies and a fuel assembly handling tool. These items should be used for rehearsal of handling evolutions in the ATR canal to aid in the maturation of handling procedures. This will provide "hands-on" experience prior to design finalization.

The analyses accomplished during the conceptual design phase are sufficient to prove viability of the overall design and irradiation campaign. Additional analyses will need to be performed in support of the final experiment safety assurance package and fuel performance considerations. These analyses are listed for each discipline area below:

- Neutronic analyses to address specific safety considerations such as reactivity cascading and irradiated shipment decay time followed by formal documentation, checking, and review of associated Engineering Calculations and Analysis Reports (ECAR).
- Thermal analyses to address specific safety considerations such as low-likelihood severe conditions including reactivity insertion, flow blockage, and accidental drop accidents followed by formal documentation, checking, and review of associated ECAR's.
- Detailed structural analyses of all components for appropriate service levels followed by formal documentation, checking, and review of associated ECAR's.
- Additional fuel performance modelling using as-built particle size distributions, 3D heat transfer model, and other refinements.

The work described above, in combination with performance of the applicable INL engineering procedures and design verification per GDE-607[19] will constitute completion of the KJRR-FAI design. Additional preparatory work for concerned facilities within the ATR complex must also be performed in advance of irradiating the KJRR fuel assembly as part of the KJRR CRADA Phase II. This work includes core modelling methods deployment, revision to facility SAR's (as needed), and nuclear characterization in the ATR critical facility. The plan for completing this work is documented elsewhere[4].

4. References

[1] Dennis D. Keiser Jr., Jan-Fong Jue, Bo Yao, Emmanuel Perez, Yongho Sohn, and Curtis R. Clark, "Microstructural characterization of U–7Mo/Al–Si alloy matrix dispersion fuel plates fabricated at 500 ˚C", Journal of Nuclear Materials 412 (2011) 90–99.

[2] "Safety Evaluation Report related to the Evaluation of Low-Enriched Uranium Silicide-Aluminum Dispersion Fuel for Use in Non-Power Reactors", NUREG-1313, U.S. Nuclear Regulatory Commission, July 1988.

[3] "LEU UMo Dispersion Fuel Tests at KAERI", INL Document Statement of Work SOW-110099, rev 2, 8-6-2013.

[4] INL Document PLN-4584, "Ki-Jang Research Reactor Fuel Assembly Irradiation in the ATR", rev 0, 12/18/2013.

[5] INL Document FOR-169, "Ki-Jang Research Reactor Fuel Assembly Irradiation Campaign", rev 0, draft December 2013.

[6] "MCNP Team, "MCNP 5.1.40 RSICC Release Notes," LA-UR-05-8617, November 10, 2005.

[7] X-5 Monte Carlo Team, "MCNP—A General Monte Carlo N-Particle Transport Code, Version 5," Volume I, LA-UR-03-1987, Los Alamos National Laboratory, April 24, 2003 (Revised 10/3/05) and Volume II, LA-CP-0245, Los Alamos National Laboratory, April 24, 2003 (Revised 10/3/05) (Vol. II is available with a licensed copy of MCNP).

[8] T. Nakagawa, et al., "Japanese Evaluated Nuclear Data Library Version 3 Revision-2: JENDL-3.2," Journal of Nuclear Science and Technology, 32, pp. 1259-1271 (December 1995).

[9] B. G. Schnitzler, "ORIGEN2 Cross Section Library Assessment for ATR Applications," BGS-6-91, EG&G Idaho Interoffice Correspondence, Idaho National Laboratory, April 4, 1991.

[10] ABAQUS Standard, Version 6.11-1, SIMULIA, Inc., Providence, RI, 2010.

[11] Hendrickson, M. B., "ATR Northeast Flux Trap Flow Rates with the MICE Facility Installed," TRA-ATR-1503, Rev. 2, June, 2001.

[12] Lee, S. H., Park, J. M., and Kim, C. K., "Thermophysical Properties of U-Mo/Al Alloy Dispersion Fuel Meats," International Journal of Thermophysics 28(5), p. 1578-1594, 2007.

[13] Polkinghorne, S. T. and Lacy, J. M., "Thermophysical and Mechanical Properties of ATR Core Materials," Document No. PG-T-91-031, August 1991.

[14] Perry, R. H., and Green, D. W., "Perry's Chemical Engineers' Handbook," 7th Edition, McGraw-Hill, 1997.

[15] KAERI Document KJ-374-KN-442-010, "KIJANG RESEARCH REACTOR Requirements of FA Irradiation Test and PIE in ATR", 07/31/2013.

[16] Polkinghorne, S. T., "Re-Analysis of ATR Loss of Commercial Power Accident," EDF-4953, Rev. 0, 2004.

[17] Knoebel, D. H., Harris, S. D., Crain, B., and Biderman, R. M., "Forced-Convection Subcooled Critical Heat Flux – D_2O and H_2O Coolant with Aluminum and Stainless Steel Heaters," Document No. DP-1306, Savannah River Laboratory, February 1973.

[18] N.E. Woolstenhulme, R.B. Nielson, and D.B. Chapman, "KJRR-FAI Hydraulic Flow Testing Input Package", INL External Report INL/EXT-13-30858, December 2013.

[19] INL Document GDE-607, "Experiment Engineering Design Process", rev 1, 4-1-2013.